Search for a space charge layer in thin film battery materials with low-energy muons

Citation for the original published paper (version of record):
Sugiyama, J., Nocerino, E., Forslund, O. et al (2023). Search for a space charge layer in thin film battery materials with low-energy muons. Journal of Physics: Conference Series, 2462(1). http://dx.doi.org/10.1088/1742-6596/2462/1/012046

(article starts on next page)

PAPER • **OPEN ACCESS**

Search for a space charge layer in thin film battery materials with low-energy muons

To cite this article: Jun Sugiyama *et al* 2023 *J. Phys.: Conf. Ser.* **2462** 012046

Journal of Physics: Conference Series **2462** (2023) 012046 doi:10.1088/1742-6596/2462/1/012046

Search for a space charge layer in thin film battery materials with low-energy muons

Jun Sugiyama[1,*], Elisabetta Nocerino[2], Ola K. Forslund[3], Yasmine Sassa[3], Martin Månsson[2], Shigeru Kobayashi[4], Kazunori Nishio[4], Taro Hitosugi[4], Andreas Suter[5], Thomas Prokscha[5]

[1] Neutron Science and Technology Center, Comprehensive Research Organization for Science and Society (CROSS), Tokai, Ibaraki 319-1106, Japan
[2] Department of Applied Physics, KTH Royal Institute of Technology, Roslagstullsbacken 21, SE-106 91 Stockholm, Sweden
[3] Department of Physics, Chalmers University of Technology, SE-412 96 Göteborg, Sweden
[4] School of Materials and Chemical Technology, Tokyo Institute of Technology, Tokyo 152-8552, Japan
[5] Laboratory for Muon Spin Spectroscopy, Paul Scherrer Institut, CH-5232 Villigen PSI, Switzerland

E-mail: `juns@triumf.ca or j_sugiyama@cross.or.jp`

Abstract. In an all solid state Li-ion battery, it is crucial to reduce ionic resistivity at the interface between the electrode and the electrolyte in order to enhance Li^+ mobility across the interface. Recent first principles calculations predict the presence of a space-charge layer (SCL) at the interface due to the difference in the Li^+ chemical potential at the interface between two different materials, as in the metal-semiconductor junction in electronic devices. However, the presence of SCL has never been experimentally observed. Our first attempt in a fresh multilayer sample, Cu(10 nm)/Li_3PO_4(50 nm)/$LiCoO_2$(100 nm) on a sapphire substrate, with low-energy μ^+SR (LE μ^+SR) revealed a gradual change in the nuclear magnetic field distribution width as a function of implantation depth even across the interface between Li_3PO_4 and $LiCoO_2$. This implies that the change in the field distribution width at SCL of the sample is too small to be detected by LE μ^+SR.

1. Introduction

The all solid-state battery, consisting of a solid cathode, solid anode, and solid electrolyte, is believed to provide a solution for several issues concerning current Li-ion batteries, as it would allow to improve safety and volumetric charge density of the current Li-ion batteries. For this reason, in recent years massive attention has been directed towards the development of all solid-state batteries from the scientific community. The most significant issue to overcome for realizing an all solid-state battery is how to control the interface layer, which is newly formed during a charge and discharge reaction, between the electrode and electrolyte. In fact, according to electrochemical analyses and ex-situ compositional analyses, such a layer, i.e., a solid-electrolyte interface (SEI), is known to exist in conventional Li-ion batteries based on liquid electrolyte [1]. A similar layer is expected to be also formed in an all solid-state battery [2].

Very recent first principles calculations highlighted the possible occurrence of a second issue [3]: the formation of a space-charge layer (SCL) at the interface between the cathode and

electrolyte due to the difference of their chemical potentials. In other words, Li vacancies are spontaneously formed in the electrolyte layer at the vicinity of the interface. Furthermore, the vacancy concentration is expected to decrease with the distance from the interface and finally become negligibly small. Such an SCL naturally increases the interfacial resistance, leading to the decrease in both the working voltage and response time for a rapid charge/discharge. In the worst case scenario, an all solid-state battery would not work at all due to the SCL.

At present, the existence of such layer has not been observed experimentally. However, empirical indications of the existence of SCL are provided, for example, by the $LiCoO_2$ battery material. Indeed, an oxide buffer layer interposed between the $LiCoO_2$ cathode and the sulfide electrolyte significantly reduces the interfacial resistance [4]. In addition, electric potential distribution measurements in an all solid-state battery ($LiCoO_2/Li_{1+x+y}Al_yTi_{2y}Si_xP_{3x}O_{12}/Li$) showed a potential gradient in the electrolyte layer within approximately 1000 nm of the interface [5]. Nevertheless, more reliable or direct evidence of the SCL is required to further improve the interface properties in an all solid-state battery.

In order to observe the SCL, a nondestructive technique with a good depth resolution is needed, since the attempt to fabricate the samples for cross-section-view observations alters and/or destroys the potential gradient at the interface. While a conventional μ^+SR is one of the powerful tools to observe the Li-distribution and diffusion in solids [6, 7], it lacks a depth resolution. We have, therefore, attempted to use a low-energy (LE) μ^+SR technique, which allows depth dependent studies with an adjustable range, by tuning the implantation energy ($E_{\rm imp}$) down to keV range [8, 9, 10, 11]. In the SCL, the relaxation rate of the transverse field (TF) oscillation spectrum is expected to decrease, due to the decreasing Li concentration. Here, TF means the magnetic field perpendicular to the initial muon spin polarization. Thus, we have mainly measured the TF-μ^+SR spectra as a function of $E_{\rm imp}$.

2. Experimental

The following two multilayers samples were prepared by a PLD technique:
♯1: Cu(10 nm)/Li_3PO_4(50 nm)/$LiCoO_2$(100 nm) on a sapphire substrate
♯2: Cu(10 nm)/Li_3PO_4(75 nm)/$LiCoO_2$(100 nm) on a sapphire substrate
The area of the sample was 10×10 mm^2. The multilayers sample was placed on the Ni coated Al plate. The LE μ^+SR spectra were measured mainly in TF with $H_{\rm TF} = 50$ Oe at temperatures between 100 and 320 K. The experimental techniques are described in more detail elsewhere [12, 13]. The obtained μ^+SR spectra were analyzed using musrfit [14].

3. Results and Discussion

Figures 1(a) and 1(b) show the volume fraction ($V_{\rm F}$) of the stopped muons as a function of $E_{\rm imp}$ in the sample ♯1 simulated with SRIM [15] and TRIMSP [16], while Fig. 1(c) shows the $E_{\rm imp}$ dependence of the TF relaxation rate ($\sigma_{\rm TF}$) at 320 K. Here, $\sigma_{\rm TF}$ was obtained by fitting the TF-μ^+SR spectra with:

$$A_0 P_{\rm TF}(t) \quad = \quad A_{\rm TF} \cos(2\pi f_{\rm TF} t + \phi_{\rm TF}) \exp(-\frac{1}{2}\sigma_{\rm TF}^2 t^2), \tag{1}$$

where A_0 denotes the initial asymmetry at $t = 0$, $P_{\rm TF}(t)$ denotes the μ^+ spin depolarization function, $A_{\rm TF}(= A_0)$ denotes the asymmetry, $f_{\rm TF}$ denotes the μ^+ spin precession frequency caused by TF, $\phi_{\rm TF}$ denotes the initial phase of the precession, and $\sigma_{\rm TF}$ denotes the Gaussian relaxation rate for the oscillatory signal and roughly corresponds to the spin-spin relaxation rate.

From the $V_{\rm F}(E_{\rm imp})$ curves simulated with SRIM [Fig. 1(a)], it is found that $V_{\rm F}^{\rm Cu} \sim 100\%$ at $E_{\rm imp} = 2$ keV, $V_{\rm F}^{\rm Li_3PO_4} \sim 100\%$ at $E_{\rm imp} = 8$ keV, and $V_{\rm F}^{\rm LiCoO_2} \sim 100\%$ at $E_{\rm imp} = 20$ keV.

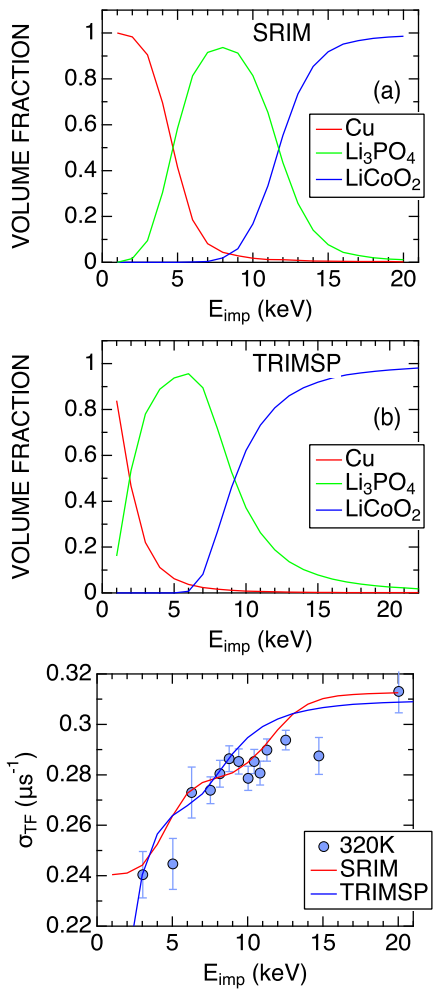

Figure 1. The volume fraction of the implanted μ^+ stopped in the three layers in the sample ♯1, Cu(10 nm)/Li_3PO_4(50 nm)/$LiCoO_2$(100 nm) on a sapphire substrate, as a function of the implantation energy ($E_{\rm imp}$) simulated with (a) SRIM [15] and (b) TRIMSP [16]. (c) the relationship between the TF relaxation rate ($\sigma_{\rm TF}$) and $E_{\rm imp}$ for the sample ♯1. In (c), the predicted $\sigma_{\rm TF}(E_{\rm imp})$ curves with SRIM and TRIMSP are also plotted.

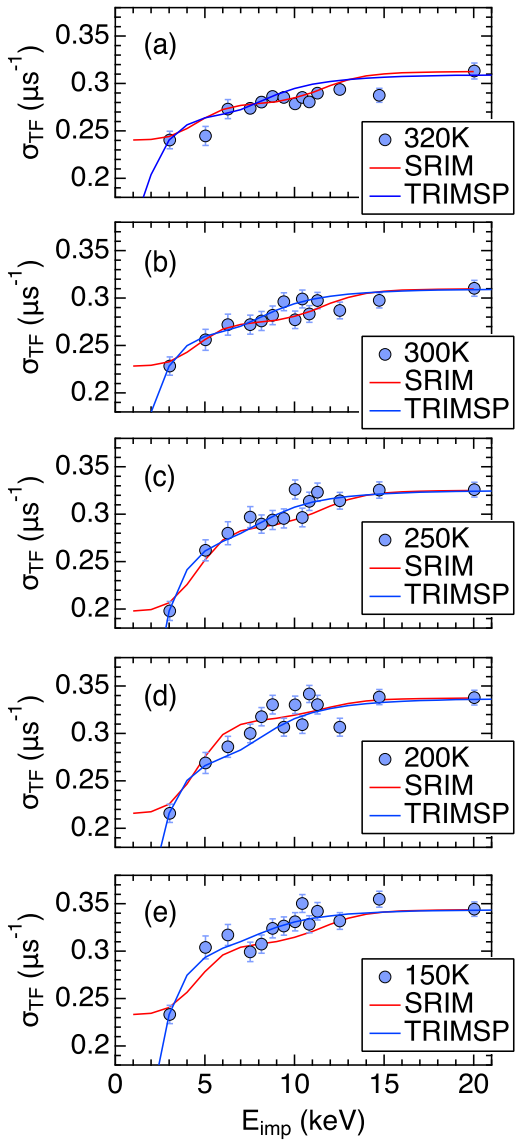

Figure 2. The $E_{\rm imp}$ dependence of $\sigma_{\rm TF}$ for the sample ♯1 measured at (a) 320 K, (b) 300 K, (c) 250 K, (d) 200 K, and (e) 150 K. Red solid lines represent the predicted dependence with SRIM, while blue solid line represents that with TRIMSP only in (a). (a) is the same to Fig. 1(c).

Therefore, using the $V_{\rm F}(E_{\rm imp})$ curves predicted with SRIM for the three components and the observed $\sigma_{\rm TF}$s at $E_{\rm imp}$ = 2, 8, and 20 keV, the $\sigma_{\rm TF}(E_{\rm imp})$ curve without SCL is obtained as [Fig. 1(c)] :

$$\begin{aligned}\sigma_{\rm TF}^{\rm preS}(E_{\rm imp}) &= V_{\rm F}^{\rm Cu}(E_{\rm imp})\sigma_{\rm TF}(2\ {\rm keV}) + V_{\rm F}^{\rm Li_3PO_4}(E_{\rm imp})\sigma_{\rm TF}(8\ {\rm keV}) \\ &+ V_{\rm F}^{\rm LiCoO_2}(E_{\rm imp})\sigma_{\rm TF}(20\ {\rm keV}). \end{aligned} \quad (2)$$

A similar procedure provides the $\sigma_{\rm TF}^{\rm preT}(E_{\rm imp})$ curve based on the TRIMSP simulation as also seen in Fig. 1(c).

Figure 2 shows the relationship between $\sigma_{\rm TF}$ and $E_{\rm imp}$ at 320, 300, 250, 200, and 150 K together with the predicted $\sigma_{\rm TF}(E_{\rm imp})$ curves based on the SRIM and TRIMSP simulations: i.e., both $\sigma_{\rm TF}^{\rm preS}(E_{\rm imp})$ and $\sigma_{\rm TF}^{\rm preT}(E_{\rm imp})$ curves. When SCL is formed, the Li content decreases in SCL. This leads to a smaller $\sigma_{\rm TF}$ in SCL than the prediction. However, it is highly unlikely to show a systematic discrepancy between the measured $\sigma_{\rm TF}(E_{\rm imp})$ and $\sigma_{\rm TF}^{\rm preS}(E_{\rm imp})$ [or $\sigma_{\rm TF}^{\rm preT}(E_{\rm imp})$] curves. In order to emphasize such discrepancy, Figs. 3 and 4 show the $E_{\rm imp}$ dependence of $\delta\sigma_{\rm TF}(= \sigma_{\rm TF} - \sigma_{\rm TF}^{\rm preS})$ and $(= \sigma_{\rm TF} - \sigma_{\rm TF}^{\rm preT})$ for the two samples. The $\delta\sigma_{\rm TF}(E_{\rm imp})$ curves do not show a sudden decrease at the interface, at which $V_{\rm F}^{\rm Li_3PO_4} = V_{\rm F}^{\rm LiCoO_2}$ based on the two simulations [Figs. 1(a) and 1(b)]. This indicates the following two possibilities:
1) SCL does not exist or 2) the thickness of SCL is too thin to be resolvable even with LE μ^+SR. Since the thickness of SCL is predicted to increase after a charge and discharge reaction [3], it would be a good idea to study the interface of the charged multilayer battery with LE μ^+SR.

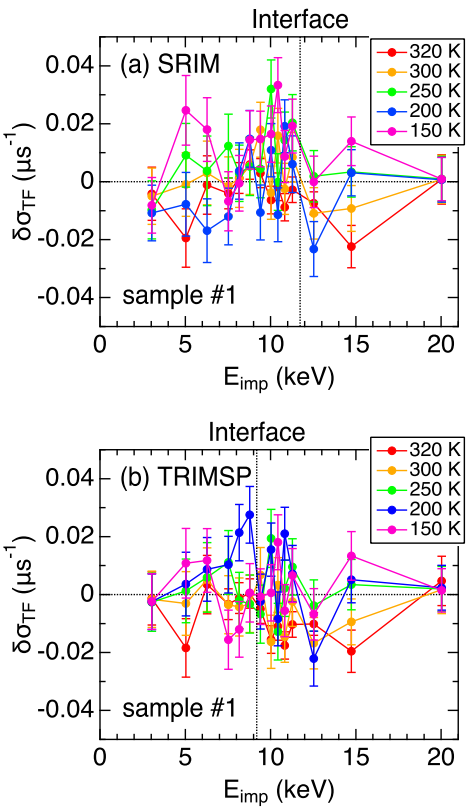

Figure 3. The $E_{\rm imp}$ dependence of the deviation of the measured $\sigma_{\rm TF}$ and predicted $\sigma_{\rm TF}$ ($\delta\sigma_{\rm TF}$) with (a) SRIM and (b) TRIMSP for the sample ♯1. Vertical dotted lines labeled "Interface" represent the $E_{\rm imp}$, at which the the volume fraction of Li_3PO_4 is equivalent to that of $LiCoO_2$ with the two simulations [see Figs. 1(a) and 1(b)].

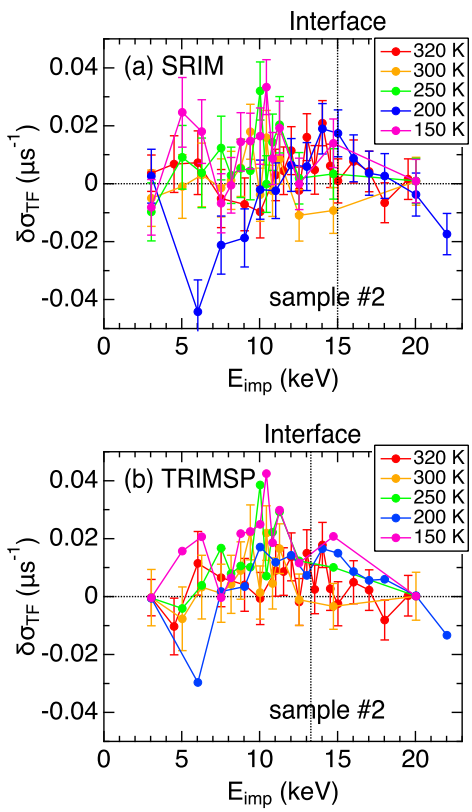

Figure 4. The $E_{\rm imp}$ dependence of the deviation of the measured $\sigma_{\rm TF}$ and predicted $\sigma_{\rm TF}$ ($\delta\sigma_{\rm TF}$) with (a) SRIM and (b) TRIMSP for the sample ♯2. Vertical dotted lines labeled "Interface" represent the $E_{\rm imp}$, at which the the volume fraction of Li_3PO_4 is equivalent to that of $LiCoO_2$ with the two simulations.

In order to study the dynamic behavior, we have also measured the ZF- and LF-μ^+SR spectra for the Li_3PO_4 layer in the sample ♯1 with $E_{\rm imp} = 8$ keV, at which $V_{\rm F}^{\rm Li_3PO_4} \sim 100\%$ predicted by SRIM (72% by TRIMSP) [see Fig. 1(a) and 1(b)]. The ZF- and LF-μ^+SR spectra were fitted with a dynamic Gaussian Kubo-Toyabe function. Figure 5 shows the temperature dependencies of the field distribution width (Δ) and the field fluctuation rate (ν) in the Li_3PO_4 layer. While Δ is roughly temperature independent in the whole temperature range measured, ν increases with temperature above 200 K, indicating the Li^+ diffusion in the Li_3PO_4 solid electrolyte. This behavior is expected to stabilize the SCL at low temperatures, although such stabilization is most unlikely to be seen in Figs. 3 and 4.

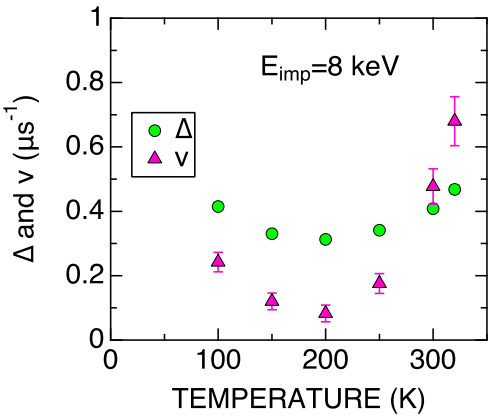

Figure 5. The temperature dependencies of the field distribution width (Δ) and field fluctuation rate (ν) in the sample ♯1 measured with $E_{\rm imp} = 8$ keV, i.e., the center of the Li_3PO_4 layer.

4. Conclusion

Even with LE μ^+SR, it was difficult to confirm the presence of SCL at the interface between the Li_3PO_4 electrolyte and $LiCoO_2$ electrode. For such purpose, it is important to make the interface at the vicinity of the surface in order to avoid the increase in the muon stopping distribution width with $E_{\rm imp}$ [17]. Moreover, it is preferable to study the interface of the sample after a charge and discharge reaction with LE μ^+SR and/or an ultra-slow muon microscope in J-PARC.

5. Acknowledgments

We thank the staff of PSI for help with the LE μ^+SR experiments (Proposal No. 20171121, No. 20180497, and No. 20190147). M.M., Y.S., and O.K.F. were partly supported by the Swedish Research Council (VR) through a neutron project grant (BIFROST, Dnr. 2016-06955). Y.S. also receive additional funding via a VR starting grant (Dnr. 2017-05078). E.N. is fully financed by the Swedish Foundation for Strategic Research (SSF) within the Swedish national graduate school in neutron scattering (SwedNess). This work was supported by the Japan Society for the Promotion Science (JSPS) KAKENHI Grant No. JP18H01863.

References

[1] Xu K 2004 *Chemical Reviews* **104** 4303–4418
[2] Kanno R 2012 private communication
[3] Haruyama J, Sodeyama K, Han L, Takada K and Tateyama Y 2014 *Chemistry of Materials* **26** 4248–4255
[4] Ohta N, Takada K, Zhang L, Ma R, Osada M and Sasaki T 2006 *Advanced Materials* **18** 2226–2229
[5] Yamamoto K, Iriyama Y, Asaka T, Hirayama T, Fujita H, Fisher C, Nonaka K, Sugita Y and Ogumi Z 2010 *Angewandte Chemie International Edition* **49** 4414–4417
[6] Sugiyama J, Mukai K, Ikedo Y, Nozaki H, Månsson M and Watanabe I 2009 *Phys. Rev. Lett.* **103**(14) 147601

[7] Månsson M and Sugiyama J 2013 *Phys. Scr.* **88** 068509
[8] Morenzoni E, Kottmann F, Maden D, Matthias B, Meyberg M, Prokscha T, Wutzke T and Zimmermann U 1994 *Phys. Rev. Lett.* **72**(17) 2793 – 2796
[9] Morenzoni E 1997 *Appl. Magn. Reson.* **13** 219 – 229
[10] Prokscha T, Birke M, Forgan E, Glückler H, Hofer A, Jackson T, Küpfer K, Litterst J, Morenzoni E, Niedermayer C, Pleines M, Riseman T, Schatz A, Schatz G, Weber H and Binns C 1999 *Hyperfine Interact.* **120-121** 569 – 573
[11] Prokscha T, Morenzoni E, Deiters K, Foroughi F, George D, Kobler R, Suter A and Vrankovic V 2008 *Nucl. Instrum. Methods Phys. Res. Sect. A* **595** 317 – 331
[12] Kalvius G M, Noakes D R and Hartmann O 2001 Handbook *on the* Physics *and* Chemistry *of* Rare Earths vol 32 (Amsterdam, Holland: North-Holland) chap 206, pp 55–451
[13] Yaouanc A and de Réotier P D 2011 Muon Spin Rotation, Relaxation, *and* Resonance, Application *to* Condensed Matter (New York: Oxford University Press)
[14] Suter A and Wojek B 2012 *Phys. Procedia* **30** 69–73 proceedings of the 12th International Conference on Muon Spin Rotation, Relaxation and Resonance (μSR2011)
[15] Ziegler J F, Ziegler M D and Biersack J P 2010 *Nuclear Instruments and Methods in Physics Research B* **268** 1818–1823
[16] Eckstein W 1994 *Radiation Effects and Defects in Solids* **130-131** 239–250
[17] Sugiyama J, Nozaki H, Umegaki I, Mukai K, Miwa K, Shiraki S, Hitosugi T, Suter A, Prokscha T, Salman Z and *et al* 2015 *Phys. Rev. B* **92**(1) 014417